

Thermally Stable Heterocyclic Imines as New Potential Nonlinear Optical Materials<sup>†</sup>Volodymyr V. Nesterov,<sup>‡</sup> Mikhail Yu. Antipin,<sup>\*,§</sup> Vladimir N. Nesterov,<sup>‡</sup> Craig E. Moore,<sup>||</sup> Beatriz H. Cardelino,<sup>⊥</sup> and Tatiana V. Timofeeva<sup>\*,‡</sup>

Department of Natural Sciences, New Mexico Highlands University, Las Vegas, New Mexico 87701, Institute of Organoelement Compounds, Russian Academy of Sciences, 28 Vavilov St., B-334, Moscow, Russia, Space Science Laboratory, NASA George C. Marshall Space Flight Center, Huntsville, Alabama 35812, and Department of Chemistry, Spelman College, Atlanta, Georgia 30314

Received: September 15, 2003; In Final Form: January 3, 2004

In the course of a search for new thermostable acentric nonlinear optical crystalline materials, several heterocyclic imine derivatives were designed, with the general structure D- $\pi$ -A(D'). Introduction of a donor amino group (D') into the acceptor moiety was expected to bring H-bonds into their crystal structures, and so to elevate their melting points and assist in an acentric molecular packing. Six heterocycle-containing compounds of this type were prepared, single crystals were grown for five of them, and these crystals were characterized by X-ray analysis. A significant melting temperature elevation was found for all of the synthesized compounds. Three of the compounds were also found to crystallize in acentric space groups. One of the acentric compounds is built as a three-dimensional H-bonded molecular network. In the other two compounds, with very similar molecular structure, the molecules form one-dimensional H-bonded head-to-head associates (chains). These chains are parallel in two different crystallographic directions and form very unusual interpenetrating chain patterns in an acentric crystal. Two of the compounds crystallized with centrosymmetric molecular packing.

## 1. Introduction

The application of organic compounds as nonlinear optical (NLO) crystalline materials is usually complicated by the requirement of their acentric crystallization, because centrosymmetric crystals have vanishing second harmonic generation (SHG) responses. There is a number of approaches that can help in obtaining acentric crystals built of achiral molecules. The conditions that control formation of acentric crystal structures are described, in particular, in the review by Gorman et al.<sup>1</sup> Another very important property of NLO chromophores is their thermal stability, characterized by their melting point (denoted as  $T_m$  or mp) and decomposition temperature (denoted as  $T_d$ ). Because melting point is usually related to both molecular structure and intermolecular interactions (molecular packing mode), it is logical to expect that intermolecular H-bonds increase the thermal stability of any organic crystal. It should be mentioned that a high temperature of decomposition of a compound is not directly interconnected with its melting point and that, actually, the application characteristics of a crystalline material cannot be improved if its melting point is low. Therefore, melting point is also an important property of NLO materials. Because intermolecular H-bonds also provide a force to override the dipole-dipole repulsions, they can be a convenient design element toward achievement of thermally stable acentric crystalline NLO materials.

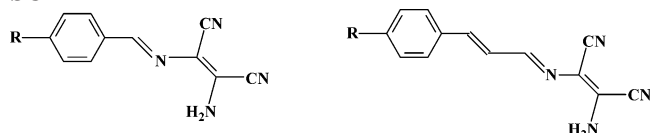
The present work is a continuation of our search for new thermally stable potential nonlinear optical materials. In our preceding work,<sup>2</sup> we have synthesized and investigated arylidene

derivatives of diaminomaleonitrile (aromatic imines) as potential NLO crystalline materials. To increase the probability of acentric crystallization of achiral imines, we introduced the electron donating amino group into the electron acceptor moieties of all the molecules. So, instead of a traditional D- $\pi$ -A structure, we synthesized compounds with a nontraditional D- $\pi$ -A(D') structure. We assumed that such "nontraditional" design would reduce the dipole moments of the molecules and their dipole-dipole repulsions, increasing the chances to obtain acentric crystals. Another useful property introduced by the NH<sub>2</sub> group was the ability to form intermolecular H-bonds in the crystals, which could result in the elevation of the melting temperatures of the compounds.

Indeed, we found<sup>2</sup> that the melting points of all compounds **1–6** (see Scheme 1 and table below) were much higher than those of similar compounds described in the literature, which do not form any H-bonds. It was also found that four out of six of the compounds investigated by X-ray analysis<sup>2</sup> crystallized in acentric space groups due to the formation of H-bonded supramolecular aggregates (chains, layers, or nets). Some characteristics of the compounds **1–6** are presented in the following table.

	mp, °C	space group; Z	$\beta$ , 10 <sup>-51</sup> C m <sup>3</sup> V <sup>-2</sup>		mp, °C	space group; Z	$\beta$ , 10 <sup>-51</sup> C m <sup>3</sup> V <sup>-2</sup>
<b>1</b>	209–210	<i>Pca</i> 2 <sub>1</sub> ; 4	54.3	<b>4</b>	211–212	<i>C2/c</i> ; 8	140.4
<b>2</b>	220–221	<i>Pna</i> 2 <sub>1</sub> ; 4	64.4	<b>5</b>	210–211	<i>Pca</i> 2 <sub>1</sub> ; 4	188.8
<b>3</b>	222–223	<i>P2<sub>1</sub>/c</i> ; 4	87.4	<b>6</b>	161–162	<i>Pca</i> 2 <sub>1</sub> ; 8	256.6

## SCHEME 1

R = HO (**1**), CH<sub>3</sub>O (**2**), (CH<sub>3</sub>)<sub>2</sub>N (**3**), (C<sub>2</sub>H<sub>5</sub>)<sub>2</sub>N (**4**) R = (CH<sub>3</sub>)<sub>2</sub>N (**5**), (C<sub>2</sub>H<sub>5</sub>)<sub>2</sub>N (**6**)<sup>†</sup> Part of the special issue "Alvin L. Kwiram Festschrift".<sup>\*</sup> To whom correspondence should be addressed. Phone: (505) 454-3362. Fax (505) 454-3103. E-mail: tvtimofeeva@nmhu.edu.<sup>‡</sup> New Mexico Highlands University.<sup>§</sup> Russian Academy of Sciences.<sup>||</sup> NASA George C. Marshall Space Flight Center.<sup>⊥</sup> Spelman College.

**TABLE 1: Summary of Crystallographic Data for Compounds 7–10 and 12**

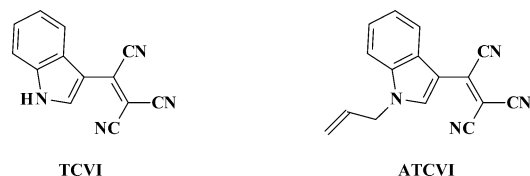
	7	7·CH <sub>3</sub> CN	8	9·0.5H <sub>2</sub> O	10	12
formula	C <sub>10</sub> H <sub>8</sub> N <sub>4</sub> S	C <sub>10</sub> H <sub>8</sub> N <sub>4</sub> S·CH <sub>3</sub> CN	C <sub>10</sub> H <sub>8</sub> N <sub>4</sub> S	C <sub>9</sub> H <sub>6</sub> N <sub>4</sub> O·0.5H <sub>2</sub> O	C <sub>13</sub> H <sub>9</sub> N <sub>5</sub>	C <sub>19</sub> H <sub>15</sub> N <sub>5</sub>
diffractometer	Enraf-Nonius	Enraf-Nonius	Enraf-Nonius	Enraf-Nonius	Enraf-Nonius	Enraf-Nonius
temperature, K	298	298	295	298	295	295
crystal system	monoclinic	monoclinic	monoclinic	orthorhombic	orthorhombic	monoclinic
space group	<i>P</i> 2 <sub>1</sub> / <i>c</i>	<i>P</i> 2 <sub>1</sub> / <i>c</i>	<i>P</i> 2 <sub>1</sub>	<i>Fdd</i> 2	<i>Pna</i> 2 <sub>1</sub>	<i>P</i> 2 <sub>1</sub> / <i>c</i>
Unit Cell Dimensions:						
<i>a</i> , Å	7.252(2)	6.631(1)	6.894(1)	24.447(5)	10.208(2)	8.437(2)
<i>b</i> , Å	22.588(5)	28.084(6)	12.355(3)	40.453(8)	22.983(5)	11.525(2)
<i>c</i> , Å	13.688(3)	7.325(2)	13.064(3)	3.815(1)	5.041(1)	16.874(3)
$\alpha$ , deg	90.00	90.00	90.00	90.00	90.00	90.00
$\beta$ , deg	103.53(3)	90.12(3)	102.27(3)	90.00	90.00	101.16(3)
$\gamma$ , deg	90.00	90.00	90.00	90.00	90.00	90.00
volume, Å <sup>3</sup>	2176.8(8)	1364.1(5)	1087.3(4)	3773(1)	1182.7(4)	1609.7(6)
<i>Z</i>	8	4	4	16	4	4
density (g cm <sup>-3</sup> )	1.320	1.253	1.321	1.374	1.321	1.293
ind reflns.	5055	1965	3391	2339	1881	4100
obsd reflns	1923	738	1687	956	1250	1270
final <i>R</i> <sub>1</sub>	0.0655	0.0790	0.0765	0.0519	0.0419	0.0645
final <i>wR</i> <sub>2</sub>	0.2022	0.2639	0.2714	0.1307	0.1213	0.1852
GOF	1.039	1.032	1.046	1.092	1.064	0.972

Rather unusual molecular packing was found in acentric crystals of compounds **5** and **6**. In these structures, the molecules form chains along two diagonal crystallographic directions. These H-bonded chains have a parquet-like molecular organization with large gaps between translationally equivalent molecules. In the crystal, these gaps are filled with the molecules belonging to the neighboring chains, and the angles between directions of the interpenetrating chains are about 60° and 70° in **5** and **6**, respectively.

Theoretical calculations of dipole moments and first-order hyperpolarizabilities ( $\beta$ ) reveal that molecules with an amino group in the donor moiety lose up to 55% of their dipole moment values and their  $\beta$ 's are reduced up to 2 times, when compared to compounds without an NH<sub>2</sub> substituent in the acceptor group. However, the values of the first hyperpolarizability still remain acceptably high for all compounds considered (see table above).

Overall, the approach to design acentric thermostable compounds by incorporating an NH<sub>2</sub> substituent to the acceptor group appears to be quite useful. Thus, we decided to apply a similar molecular and crystal design to a series of heterocycle-containing imine derivatives of diaminomaleonitrile. It should be mentioned that the possibility of incorporating heterocyclic rings into potential nonlinear optical chromophores has been already investigated in a number of articles.<sup>3–12</sup> In none of these investigations, however, a nontraditional molecular structure design has been used.

In the present work, we concentrated on crystalline materials utilizing the proposed design to obtain acentric crystals with high thermal stability, built from heterocycle-containing polarized molecules. In our preceding paper<sup>2</sup> we have discussed the influence of intermolecular H-bonds on the thermal stability of crystalline materials. It was reported that, in pairs of analogous compounds with and without intermolecular hydrogen bonds, the difference in *T*<sub>m</sub> might be higher than 70°. Lately we found an example of an even more dramatic difference in *T*<sub>m</sub> values between similar compounds: 3-tricyanovinylindole<sup>13</sup> (TCVI) forms intermolecular H-bonds and its melting point is equal to



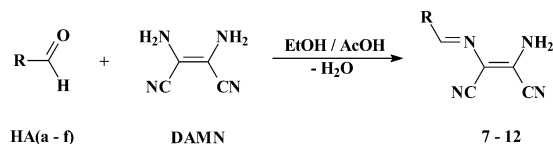
275–276 °C, whereas 1-allyl-3-tricyanovinylindole<sup>14</sup> (ATCVI) does not possess any active hydrogen atoms for H-bond formation, and it melts at 145–146 °C.

As was already mentioned, in the present study we chose to investigate heterocyclic imine derivatives of diaminomaleonitrile. Traditional and nontraditional molecular designs are presented in Scheme 2a,b, respectively (an indole ring is shown as an example of a heterocyclic donor group).

**SCHEME 2**

To confirm the expected changes in the molecular electronic properties of the investigated compounds, we carried out molecular modeling and evaluation of the NLO activity of two series of heterocyclic imine derivatives of diaminomaleonitrile (one with and another without active H atoms for H-bond formation). We also synthesized the series of molecules with active H atoms for H-bond formation, we evaluated their absorption spectra and thermal stability, and we characterized their molecular and crystal structure.

It should be mentioned that none of these compounds have been synthesized before; the general scheme of synthesis is presented below:

**SCHEME 3**

here R = 3-methylthiophene (**7**), 5-methylthiophene (**8**), furan (**9**), indole (**10**), benzothiophene (**11**), N-ethylcarbazole (**12**)

As donor groups (R), we used different substituted heterocycles such as thiophene, furan, indole, benzothiophene, and carbazole. In the present study, six compounds were synthesized and characterized. For five of them, crystals suitable for single-crystal X-ray analysis were grown and their structures were solved and described (see Table 1).

## 2. Experimental Section and Computational Details

**General Method of Synthesis.** Heterocyclic imines **7–12** were obtained by the reaction of heterocyclic aldehydes (Scheme 3) with diaminomaleonitrile on heating in an ethyl alcohol solution in the presence of catalytic amounts of acetic acid.<sup>15,16</sup> Heterocyclic aldehydes **HAA–f**, diaminomaleonitrile (DAM), and all solvents were purchased from Aldrich and used as received. The solution of 0.005 mol of diaminomaleonitrile (DAM) and 0.005 mol of the corresponding heterocyclic aldehyde **HAA–f** with 0.1 mL of acetic acid in 30 mL of ethanol was heated to boiling over 1–3 min. Then the reaction mixture was left to settle at room temperature overnight. The precipitates were filtered and washed with cold ethanol and then recrystallized to wash out all impurities. Structures of all imines have been characterized by <sup>1</sup>H and <sup>13</sup>C NMR spectra (Bruker, 300 MHz). Yields, melting points, and NMR spectral data for the following compounds are presented below.

**(2Z)-2-Amino-3-[(1E)-(3-methylthien-2-yl)methylene]amino}but-2-enedinitrile (**7**).** After recrystallization from ethanol, compound **7** was obtained as a yellow solid with 91% yield (0.98 g): mp 207–208 °C; <sup>1</sup>H NMR (DMSO-*d*<sub>6</sub>, 300 MHz)  $\delta$  7.46 (s, 1H), 6.84 (d, *J* = 4.78 Hz, 1H), 6.69 (bs, 2H), 6.11 (d, *J* = 4.78 Hz, 1H), 1.51 (s, 3H) ppm; <sup>13</sup>C NMR (DMSO-*d*<sub>6</sub>, 75 MHz)  $\delta$  147.7, 147.6, 143.3, 135.1, 131.6, 125.5, 114.6, 113.8, 103.5, 13.8 ppm.

**(2Z)-2-Amino-3-[(1E)-(5-methylthien-2-yl)methylene]amino}but-2-enedinitrile (**8**).** After recrystallization from acetonitrile, compound **8** was obtained as a yellow solid with 76% yield (0.82 g): mp 219–220 °C; <sup>1</sup>H NMR (DMSO-*d*<sub>6</sub>, 300 MHz)  $\delta$  7.47 (s, 1H), 6.72 (bs, 2H), 6.70 (d, *J* = 3.68 Hz, 1H), 6.05 (d, *J* = 3.68 Hz, 1H), 1.64 (s, 3H) ppm; <sup>13</sup>C NMR (DMSO-*d*<sub>6</sub>, 75 MHz)  $\delta$  149.2, 146.9, 139.4, 134.6, 127.3, 125.4, 114.6, 113.9, 103.1, 15.7 ppm.

**(2Z)-2-Amino-3-[(1E)-2-furylmethylene]amino}but-2-enedinitrile (**9**).** After recrystallization from acetonitrile, compound **9** was obtained as a yellow solid with 87% yield (0.81 g): mp 157–158 °C; <sup>1</sup>H NMR (DMSO-*d*<sub>6</sub>, 300 MHz)  $\delta$  7.18 (s, 1H), 7.06 (d, *J* = 1.47 Hz, 1H), 6.88 (bs, 2H), 6.37 (d, *J* = 3.31 Hz, 1H), 5.83 (q, *J* = 1.84 Hz, 1H) ppm; <sup>13</sup>C NMR (DMSO-*d*<sub>6</sub>, 75 MHz)  $\delta$  151.5, 147.1, 143.1, 126.3, 117.7, 114.5, 113.7, 113.1, 103.2 ppm.

**(2Z)-2-Amino-3-[(1E)-1H-indol-3-ylmethylene]amino}but-2-enedinitrile (**10**).** After recrystallization from ethanol, compound **10** was obtained as a dark-yellow solid with 94% yield (1.10 g). mp 217–218 °C; <sup>1</sup>H NMR (DMSO-*d*<sub>6</sub>, 300 MHz)  $\delta$  8.58 (bs, 1H), 7.59 (s, 1H), 7.52 (d, *J* = 7.72 Hz, 1H), 7.18 (s, 1H), 6.51 (d, *J* = 8.09 Hz, 1H), 6.30 (d, *J* = 6.62 Hz, 1H), 6.26 (bs, 2H), 6.22 (d, *J* = 6.99 Hz, 1H) ppm; <sup>13</sup>C NMR (DMSO-*d*<sub>6</sub>, 75 MHz)  $\delta$  152.5, 137.4, 135.3, 124.3, 123.3, 123.0, 122.8, 121.5, 115.3, 114.7, 114.4, 112.0, 106.0 ppm.

**(2Z)-2-Amino-3-[(1E)-1-benzothien-3-ylmethylene]amino}but-2-enedinitrile (**11**).** After recrystallization from acetonitrile, compound **11** was obtained as an orange solid with 78% yield (0.98 g): mp 194–195 °C; <sup>1</sup>H NMR (DMSO-*d*<sub>6</sub>, 300 MHz)  $\delta$  7.98 (m, *J* = 2.58, 2.94, 3.68 Hz, 1H), 7.74 (d, *J* = 11.77 Hz, 2H), 7.17 (m, *J* = 2.58, 2.94, 3.68 Hz, 1H), 6.89 (bs, 2H), 6.61 (m, *J* = 1.84, 3.68, 4.05, 5.14, 5.52 Hz, 2H) ppm; <sup>13</sup>C NMR (DMSO-*d*<sub>6</sub>, 75 MHz)  $\delta$  151.3, 140.0, 138.3, 135.2, 132.9, 126.1, 125.7, 125.6, 122.8, 114.6, 113.8, 103.9 ppm.

**(2Z)-2-Amino-3-[(1E)-(9-ethyl-9H-carbazol-3-yl)methylene]amino}but-2-enedinitrile (**12**).** After recrystallization from ethanol, compound **12** was obtained as a yellow solid with 96% yield (1.50 g): mp 213–214 °C; <sup>1</sup>H NMR (DMSO-*d*<sub>6</sub>, 300 MHz)  $\delta$  7.96 (d, *J* = 1.47 Hz, 1H), 7.54 (s, 1H), 7.30 (dt, *J* =

1.47, 6.98 Hz, 2H), 6.91 (bs, 2H), 6.78 (dd, *J* = 2.21, 8.09, 8.45 Hz, 2H), 6.62 (m, *J* = 1.11, 1.47, 5.88, 6.98 Hz, 1H), 6.39 (dt, *J* = 0.73, 6.98, 7.36 Hz, 1H), 3.59 (dt, *J* = 6.62, 6.98, 7.36 Hz, 2H), 0.44 (t, *J* = 6.98, 7.36 Hz, 3H) ppm; <sup>13</sup>C NMR (DMSO-*d*<sub>6</sub>, 75 MHz)  $\delta$  156.0, 141.7, 140.1, 127.0, 126.8, 126.4, 125.4, 122.5, 122.4, 120.6, 119.7, 114.8, 114.0, 109.7, 109.4, 103.6, 37.2, 13.8 ppm.

**Crystal Growth and X-ray Analysis.** Single crystals, suitable for X-ray analysis, were obtained for most of the compounds studied by slow evaporation of a solution containing the compound. Namely, crystals of compounds **10** and **12** have been grown from ethanol solutions, crystals of **8** from an acetonitrile solution, and those of **7** were obtained from both ethanol (hereinafter denoted as **7**) and acetonitrile (hereinafter denoted as **7**·CH<sub>3</sub>CN), giving the latter a solvate. Crystals of **9** have been grown from the reaction mixture (ethanol solution containing some water that was obtained as a product of the condensation reaction), resulting in the formation of a hydrate; there is one water molecule per two molecules of heterocyclic imine (hereinafter this hydrate will be denoted as **9**·0.5H<sub>2</sub>O).

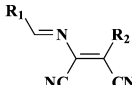
Unit cell parameters and intensities of reflections were measured using Mo K $\alpha$  radiation and the  $\theta/2\theta$  scan technique on an Enraf-Nonius CAD4 diffractometer<sup>17</sup> at room temperature. The structures were solved by a direct method. All non-hydrogen atoms were refined anisotropically. In all structures of heterocyclic imines, the hydrogen atoms were placed in the geometrically calculated positions and refined using a “riding” model. Hydrogen atoms in the solvent molecules of structures **7**·CH<sub>3</sub>CN and **9**·0.5H<sub>2</sub>O were located from a difference Fourier synthesis and included in the refinement in the isotropic approximation. Details of data collection and structure refinement are summarized in Table 1.

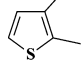
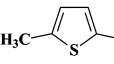
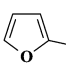
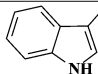
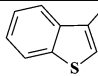
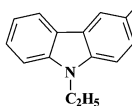
**Computational Evaluation of Molecular Structure and Hyperpolarizability.** The structures for the series of compounds presented in Scheme 3 were modeled using molecular mechanics (MM3). Theoretical calculations of hyperpolarizability that we performed in our previous investigations showed that the results obtained from semiempirical methods were in good agreement with those obtained from ab initio calculations.<sup>18,19</sup> Therefore, in this work, we used semiempirical methods for a fast evaluation of the molecular electronic properties of the investigated compounds. Theoretical calculations of the dipole moments ( $\mu$ , D), first-order hyperpolarizability ( $\beta$ , 10<sup>−51</sup> C m<sup>3</sup> V<sup>−2</sup>), and second-order hyperpolarizability ( $\gamma$ , 10<sup>−61</sup> C m<sup>4</sup> V<sup>−3</sup>) have been carried out using the modified MOPAC<sup>20</sup> and HYPER<sup>21,22</sup> programs (Table 2). The wavelengths of maximum absorbance for the investigated compounds ( $\lambda_{\text{max}}$ , nm) have been measured in THF solutions with a Hewlett-Packard UV–vis spectrophotometer and presented in Table 3.

## 3. Results and Discussion

Results from the computational evaluation of dipole moments, first- and second-order hyperpolarizabilities of a series of heterocyclic imines, with traditional and nontraditional structures (Scheme 3), are presented in Table 2. It follows from this table that the  $\beta$  values increase in the series of compounds **7–12**, which indicates that the strength of the donor moieties grows from substituted thiophene to substituted carbazole derivatives. Transition from the traditional D- $\pi$ -A structure to the nontraditional D- $\pi$ -A(D') (Scheme 3) results in some drop in the dipole moment magnitudes (up to 40%) and a decrease in the  $\beta$  values (up to 2 times). Interestingly, donor substitution into the acceptor group of the molecule changes the second-



**TABLE 2:** Calculated Molecular Electronic Properties for Heterocyclic Imines with Both Traditional and Nontraditional Structures (Dipole Moments  $\mu$  and Molecular  $\beta$  and  $\gamma$  Values)


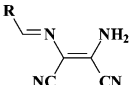
	R <sub>1</sub>	R <sub>2</sub>	$\mu$ , D	$\beta$ , $10^{-51}$ C m <sup>3</sup> V <sup>-2</sup>	$\gamma$ , $10^{-61}$ C m <sup>4</sup> V <sup>-3</sup>
7		NH <sub>2</sub>	5.31	34.3	12.6
		H	5.65	45.8	11.4
		CN	6.33	60.9	10.7
8		NH <sub>2</sub>	5.76	40.8	15.1
		H	6.04	55.0	13.9
		CN	6.49	75.1	13.7
9		NH <sub>2</sub>	4.94	45.5	11.7
		H	5.29	54.7	11.6
		CN	6.14	73.2	11.7
10		NH <sub>2</sub>	6.79	70.7	17.9
		H	8.00	82.5	16.8
		CN	9.46	113.1	16.9
11		NH <sub>2</sub>	5.40	90.2	23.7
		H	6.39	107.1	22.8
		CN	7.53	156.5	26.2
12		NH <sub>2</sub>	7.25	98.8	34.4
		H	8.22	127.6	37.4
		CN	9.27	196.7	52.1

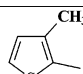
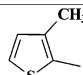
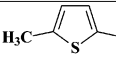
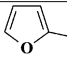
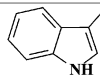
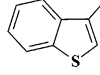
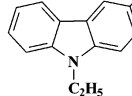
order hyperpolarizability  $\gamma$  less significantly than the  $\beta$ 's (Table 2). Computational evaluation shows that the change of dipole moments may not be sufficiently large to suppress antiparallel orientation of the molecules in the crystal. On the other hand, the changes of  $\beta$ 's show that introduction of the amino group still results in rather high values.

It could be mentioned that the results we obtained for heterocyclic imines are very similar to those for our preceding group of compounds—aromatic imines.<sup>2</sup> In the latter case, we found comparable differences in dipole moments, as well as, first- and second-order hyperpolarizability values, between traditional D- $\pi$ -A and nontraditional D- $\pi$ -A(D'). Therefore, it is possible to assume that this particular modification of molecular structure generally leads to a predictable change of molecular electronic properties of potential NLO chromophores.

One of the reasons to choose diaminomaleonitrile (DAM) as a reagent for the synthesis of designed heterocyclic imines with nontraditional D- $\pi$ -A(D') structures is that it has two amino groups, one of which reacts with carbonyl compounds, forming a carbon–nitrogen double bond. The second amino group is not active under the reaction conditions, most probably because of the strong conjugation with the  $\pi$ -system of the formed imine. Both hydrogens of this “free” amino group can participate in formation of intermolecular hydrogen bonds in the crystal. Another reason is that diaminomaleonitrile has two strong electron-withdrawing cyano groups that produce a strong acceptor moiety of the product imine. Both nitrogens of the two cyano groups can also participate in the formation of intermolecular hydrogen bonds and influence the thermal properties and crystal acentricity of the compounds.

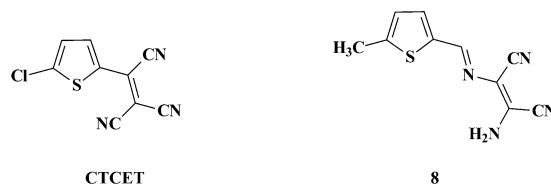
All heterocyclic imines were obtained in high yields. Reactions between heterocyclic aldehydes and diaminomaleonitrile were promoted by an acid catalyst. General information about the synthesized compounds 7–12 is listed in Table 3. It is obvious that for the synthesized compounds with intermolecular

**TABLE 3:** General Information about the Compounds Synthesized (Melting/Decomposition Temperatures, Dipole Moments  $\mu$ , Molecular  $\beta$  and  $\gamma$ ,  $\lambda_{\max}$  Values, and Crystal Colors)


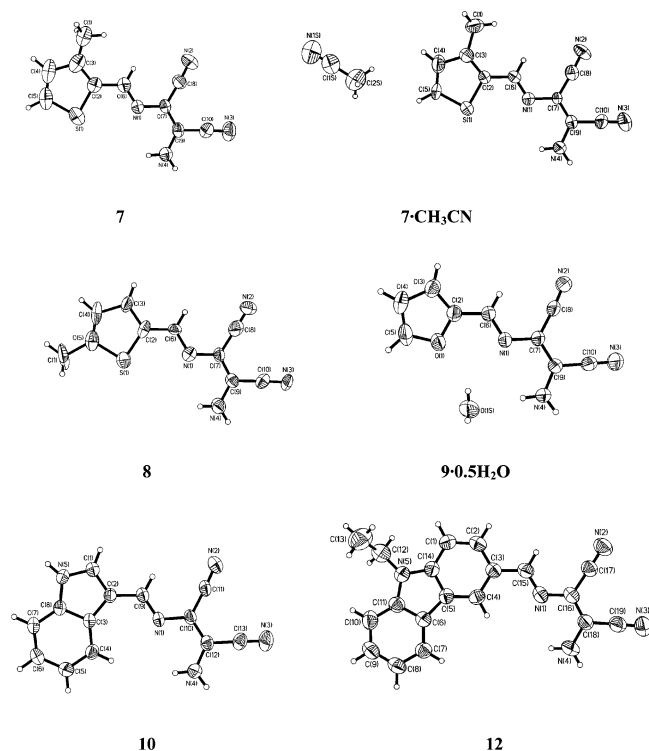
Product	R—	Melting Point, °C	$\mu$ , D	$\beta$ , $10^{-51}$ C m <sup>3</sup> V <sup>-2</sup>	$\gamma$ , $10^{-61}$ C m <sup>4</sup> V <sup>-3</sup>	$\lambda_{\max}$ , nm	Crystal color
7 <sup>‡</sup>		207–208	5.31	34.3	12.6	384	Yellow
7 <sup>•</sup> CH <sub>3</sub> CN <sup>‡</sup>		Solvent evaporates at RT*	5.31*	34.3*	12.6*	384	Yellow
8 <sup>‡</sup>		219–220	5.76	40.8	15.1	387	Yellow
9 <sup>•</sup> 0.5H <sub>2</sub> O <sup>‡</sup>		157–158*	4.94	45.5	11.7	374	Yellow
10 <sup>‡</sup>		217–218	6.79	70.7	17.9	379	Yellow
11		194–195	5.40	90.2	23.7	373	Orange
12 <sup>‡</sup>		213–214	7.25	98.8	34.4	395	Yellow

<sup>‡</sup> Compound that crystallizes in acentric space group. <sup>‡</sup> Compound that crystallizes in centrosymmetric space group. <sup>‡</sup> Temperature of decomposition. <sup>•</sup> The molecular electronic properties for 7•CN<sub>3</sub>CN are for the imine molecule 7 itself. \* In the 7•CH<sub>3</sub>CN crystal, acetonitrile solvent evaporates at room temperature (RT) during several days; the remaining compound melts at melting point of imine 7 (207–208 °C).

hydrogen bonds, we observed enhancement of the melting points in comparison to similar compounds without such bonds. For instance, 2-chloro-5-(tricyanoethenyl)thiophene<sup>23</sup> (CTCET) has a melting point of 130–131 °C. This melting point is 90° lower than for our compound 8 (mp 219–220 °C), which has just a slightly different structure (see Table 3).



**Molecular and Crystal Structure of the Compounds Studied.** An X-ray investigation of compounds 8, 9•0.5H<sub>2</sub>O, and 10 revealed that they form acentric crystals, whereas compounds 7, 7•CH<sub>3</sub>CN, and 12 form centrosymmetric structures (Table 1). All molecules studied (Figure 1) have similar geometry parameters and have planar or almost planar structures, which are favorable for an effective conjugation between the donor and acceptor parts of the molecules, and for an enhancement of the molecular NLO properties. The dihedral angles between the two planar parts of the molecules (heterocycle and aminoiminomaleonitrile fragment) are equal to 1.4° for 7 and 4.6° for two independent molecules (7A and 7B, respectively);



**Figure 1.** General view of all molecules investigated by X-ray analysis. The non-H atoms are shown with displacement ellipsoids drawn at the 50% probability level.

0.5° for **7**·CH<sub>3</sub>CN; 1.7° and 2.2° for two independent molecules of **8** (**8A** and **8B**, respectively); 3.4° for **9**·0.5H<sub>2</sub>O; 5.7° for **10**; and 6.8° for **12** (the ethyl substituent on the carbazole ring excluded from the planar fragment). The distribution of bond lengths in the investigated molecules indicates the existence of resonance between different parts of the molecules. Namely, a noticeable elongation of the double bonds and a shortening of the single bonds along the conjugated chains (so-called leveling of bonds) occurs in all structures but is more pronounced in the more polar molecules. Overall, the geometry parameters in the molecular structures of the compounds studied have the standard values for such types of compounds.<sup>24</sup> We analyzed the packing features of the six crystals studied, and the results follow.

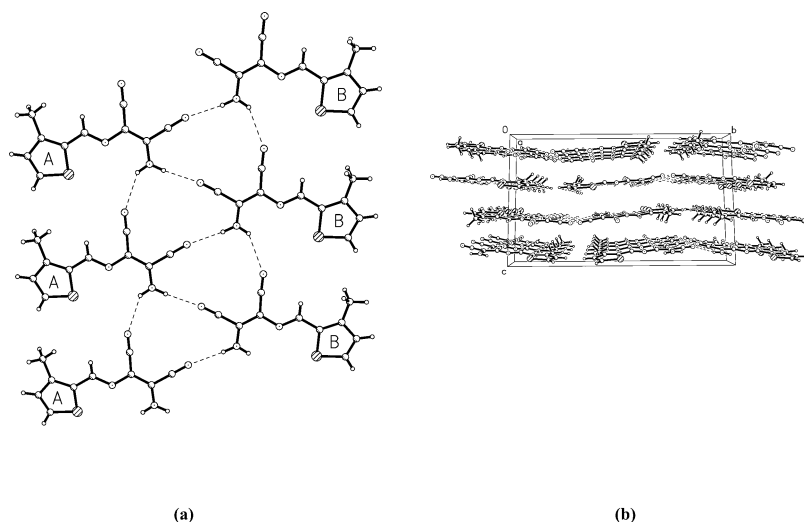
In the crystal of compound **7**, there are two symmetrically independent molecules (**A** and **B**) with similar geometries in

the unit cell. The molecules in the crystal form planar ribbons parallel to the *a*-axis, where independent molecules **A** and **B** form two parallel strings and are linked in the ribbon by intermolecular H-bonds of the N—H···N≡C type (Figure 2a, Table 4). Both hydrogens of the amino group form H-bonds with nitrogens of cyano groups of two different neighboring molecules, forming adjacent 14-membered rings (Figure 2, Table 4). Due to the presence of two symmetrically independent molecules, ribbons in the crystal are built by only translational symmetry operations. Superposition of the neighboring molecular ribbons in the crystal, where the interplanar distance is equal to 3.5 Å, is shown in Figure 2b.

In the crystal, the **7**·CH<sub>3</sub>CN molecules form ribbons parallel to the *c*-axis, where the H-bonds have the same pattern as in crystal **7**. Molecular ribbons are built by an operation that includes a glide plane *c*. The main difference of this crystal structure from the previous one is the presence of solvent molecules in the ratio 1:1. Solvent acetonitrile molecules form independent molecular stacks (Figure 3a). It should be mentioned that there are no H-bonds that link molecules of solvent to the imine molecules. Most probably because solvent molecules are located in individual channels (Figure 3), they can easily leave the crystal. Crystals **7**·CH<sub>3</sub>CN appeared to be unstable even at room temperature due to the constant loss of solvent. To run the X-ray diffraction experiment, we had to plaster the crystal with glue to slow the rate of crystal decomposition. Superposition of several neighboring molecular ribbons in the crystal, where the interplanar distance is equal to 3.4 Å, is shown in Figure 3b.

The crystal structures of **7** and **7**·CH<sub>3</sub>CN closely resemble those of compounds **3** and **4** that we mentioned in the Introduction.<sup>2</sup> All of these compounds form very similar molecular ribbons with an identical system of intermolecular H-bonds and have similar mutual orientation of ribbons in the crystal (compare Figures 2 and 3). The only distinctive feature of **7**·CH<sub>3</sub>CN is the presence of the solvent molecules in the crystal. Therefore, it is not surprising that all crystals built with similar molecular associates form similar crystal packings, having a centrosymmetric structure.

In crystal **12** molecules form planar ribbons parallel to the (101) plane, in which the molecules are linked by two intermolecular H-bonds of the N—H···N≡C type (Figure 4a, Table 4). The ribbons in the crystal of **12** are built by an operation that includes a screw axis 2<sub>1</sub>. It should be mentioned that the molecular ribbons found in the crystal of **12** are different

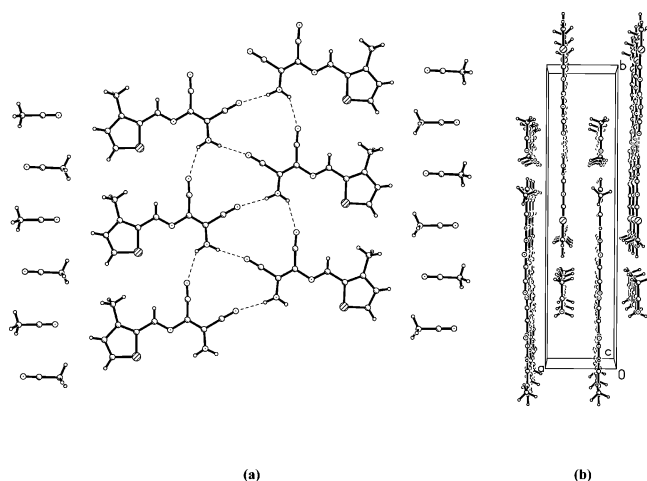


**Figure 2.** (a) fragment of one ribbon in the crystal of **7**. (b) Mutual orientation of ribbons in the unit cell along the *a*-axis.

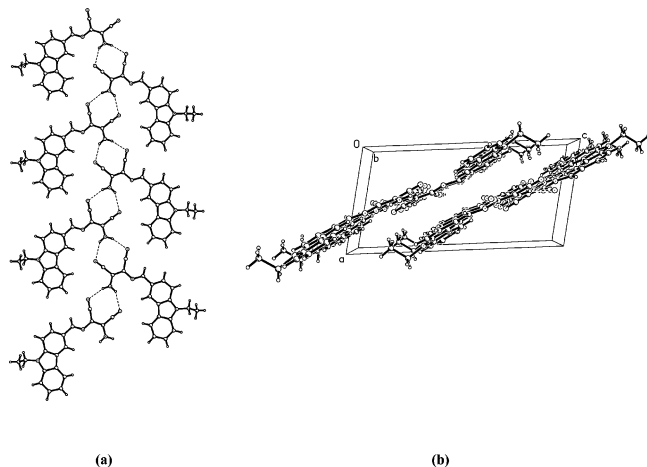
TABLE 4: Parameters of H-Bonds in Investigated Compounds

	D—H···A	symmetry	D—H	H···A	D···A	angle D—H···A
<b>7<sup>a</sup></b>	N(4)—H(4A)···N(2)	$-1 + x, y, z$	0.86	2.47	3.166(4)	138
	N(4)—H(4B)···N(3')	$-x, 0.5 + y, 0.5 - z$	0.86	2.21	3.049(4)	165
	N(4')—H(4'A)···N(2')	$1 + x, y, z$	0.86	2.37	3.083(4)	141
	N(4')—H(4'B)···N(3)	$1 - x, -0.5 + y, 0.5 - z$	0.86	2.21	3.058(4)	169
<b>7·CH<sub>3</sub>CN</b>	N(4)—H(4A)···N(2)	$x, y, -1 + x$	0.86	2.33	3.043(8)	141
	N(4)—H(4B)···N(3)	$x, -0.5 - y, -0.5 + z$	0.86	2.15	3.005(8)	172
	N(4)—H(4A)···N(3)	$1 - x, -0.5 + y, -z$	0.86	2.51	3.241(2)	143
<b>8<sup>a</sup></b>	N(4)—H(4B)···N(2')	$1 - x, 0.5 + y, -z$	0.86	2.35	3.021(2)	135
	N(4')—H(4'A)···N(3')	$2 - x, 0.5 + y, 1 - z$	0.86	2.56	3.235(2)	137
	N(4')—H(4'B)···N(2)	$2 - x, -0.5 + y, 1 - z$	0.86	2.40	3.066(2)	135
	O(1S)—H(1S)···O(1)	$x, y, z$	0.75(4)	2.35(4)	3.034(4)	152(3)
<b>9·0.5H<sub>2</sub>O</b>	N(4)—H(4A)···O(1S)	$x, y, z$	0.86	2.26	3.113(4)	174
	N(4)—H(4B)···N(2)	$-0.25 + x, -0.25 - y, -0.75 + z$	0.86	2.24	3.067(4)	163
	N(4)—H(4B)···N(2)	$-0.5 + x, 0.5 - y, -1 + z$	0.86	2.17	3.034(4)	179
<b>10</b>	N(5)—H(5A)···N(3)	$1.5 - x, 0.5 + y, 0.5 + z$	0.86	2.38	3.133(4)	147
	N(4)—H(4A)···N(3)	$1 - x, -0.5 + y, 0.5 - z$	0.86	2.39	3.140(4)	146
	N(4)—H(4B)···N(2)	$1 - x, -0.5 + y, 0.5 - z$	0.86	2.26	3.070(4)	156

<sup>a</sup> H-bond parameters for compounds **7** and **8** are presented for two independent molecules respectively.

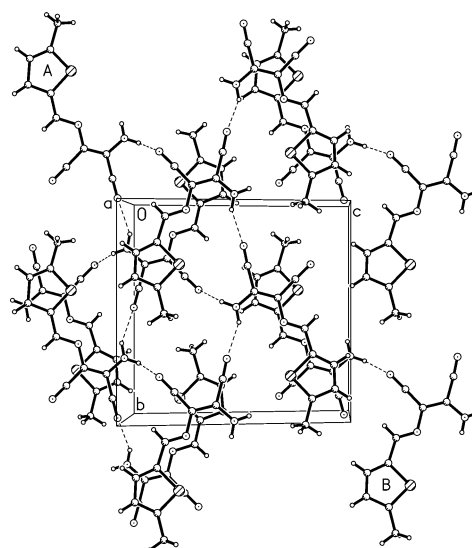


**Figure 3.** (a) Fragment of one ribbon in the crystal of **7·CH<sub>3</sub>CN**. (b) Mutual orientation of ribbons in the unit cell along the *c*-axis.



**Figure 4.** (a) Fragment of one ribbon in the crystal of compound **12**. (b) Mutual orientation of ribbons in the unit cell parallel to plane (101).

from those in **3**, **4**, **7**, or **7·CH<sub>3</sub>CN**. In this crystal, two hydrogens of the amino group of the reference imine molecule form H-bonds with two nitrogens of the cyano groups of an adjacent imine molecule, and so on. Most probably, ribbons different from those found in **3**, **4**, **7**, and **7·CH<sub>3</sub>CN** are formed due to the large size of the *N*-ethylcarbazole substituent in molecule **12**. Superposition of the two neighboring molecular ribbons in the crystal, where the interplanar distance is equal to 3.5 Å, is

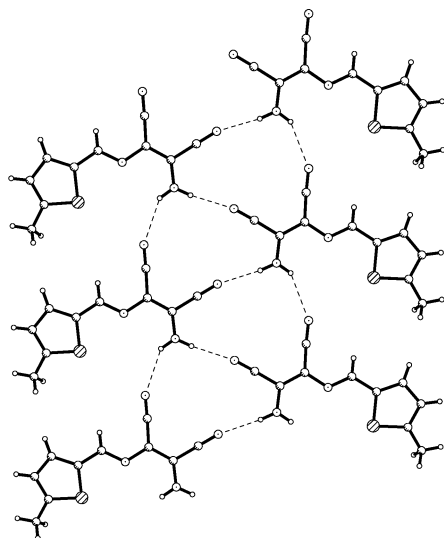


**Figure 5.** Crystal packing of compound **8** along the *a*-axis.

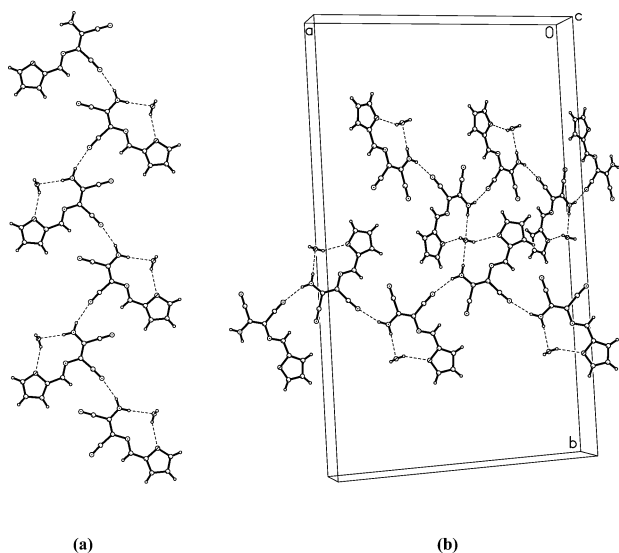
shown in Figure 4b. Despite the dissimilarity of the ribbons in **3**, **4**, **7**, **7·CH<sub>3</sub>CN**, and **12**, in all cases they do not have intermolecular gaps, are coplanar, and form centrosymmetric structures.

There are two symmetrically independent molecules (**A** and **B**) with similar geometries in the unit cell of compound **8**. The crystal packing can be described as a 3D network (Figure 5) where molecules are connected with H-bonds. Both hydrogens of the amino group form H-bonds with nitrogens of the cyano groups of two different molecules. The hydrogen bond parameters are presented in Table 4.

Interestingly, even though the difference between the molecular structures of compounds **7** and **8** is defined only by the position of one methyl group, it plays a crucial role in the determination of the crystal packing of these compounds. Theoretically, it should be possible to aggregate molecules **8** into the same ribbons as **7**, because the change in position of the methyl group (from position 3 to position 5) in the furan ring does not bring any significant steric strain to the crystal packing (Figure 6). Careful examination of the electronic factors, which also could affect the crystal structure, revealed only minor differences between the partial charges on the different atoms in molecules **7** and **8**. Therefore, it could be assumed, that the combination of the two above-mentioned factors (the position of the methyl group and the atomic charges), as well as some



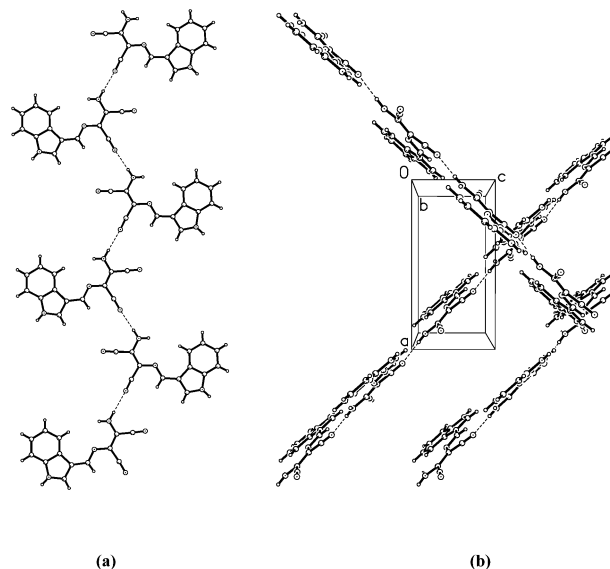
**Figure 6.** Fragment of one imaginary molecular ribbon built of molecules **8**.



**Figure 7.** (a) Fragment of one chain in the crystal of **9**·0.5H<sub>2</sub>O. (b) Mutual orientation of chains in the unit cell parallel to planes (301) and (301) for two different chains, respectively.

other factors that we were not able to identify, are responsible for the preference of one or another crystal packing pattern.

An unusual type of molecular packing, but the one that we already described in our previous paper<sup>2</sup> for molecules **5** and **6**, was found in the crystal **9**·0.5H<sub>2</sub>O. In this structure the molecules form chains parallel to two diagonal planes (301) and (301), respectively. The molecular chains are built by an operation that includes a diamond plane *d*. These H-bonded chains have a parquet-like molecular arrangement with big gaps between translational molecules on both sides of the chain (Figure 7a). These gaps are filled with the molecules belonging to the other chains related to the reference one by the axis 2. The angle between interpenetrating chains is about 55° (Figure 7b). Three symmetrically nonequivalent intermolecular hydrogen bonds were found in this crystal. One H-bond is formed between a hydrogen atom of the amino group and the nitrogen atom of the cyano group. Two other hydrogen bonds are formed with a water molecule: an oxygen atom of the water molecule forms a H-bond with the second hydrogen atom of the amino group of the imine **9**, and a hydrogen atom of the water molecule forms H-bond with the oxygen atom of the furan ring (Table



**Figure 8.** (a) Fragment of one chain in the crystal of **10**. (b) Mutual orientation of chains in the unit cell parallel to planes (201) and (201) for two different chains, respectively.

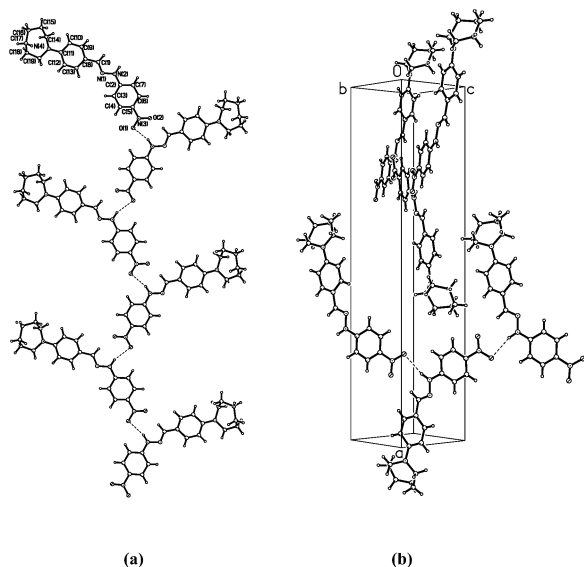
4). Due to the hydrogen bond formation, such hydrate is quite stable at room temperature for an indefinite time: it decomposes only when the substance is heated above 158 °C. This is a dramatic difference between the crystals of **9**·0.5H<sub>2</sub>O and those of **7**·CH<sub>3</sub>CN, where H-bonds between solvent and host molecules are not formed and the solvent has a trend to “evaporate” from the crystal of **7**·CH<sub>3</sub>CN. It also could be mentioned, that chains of molecules **9**·0.5H<sub>2</sub>O are linked to each other by hydrogen bonds via water molecules.

The crystal structure of **10** is similar to the crystal structure of **9**·0.5H<sub>2</sub>O. Molecules **10** in the crystal also form two identical chains (Figure 8a) parallel to two planes (201) and (201). These molecular chains are built by an operation that includes a glide plane *a*. There is an intermolecular H-bond that links molecules **10** in chains: a hydrogen of the amino group forms a H-bond with a nitrogen of a cyano group. Such chains are very similar to those found in **5** and **6**. The gaps in each chain are filled with the molecules belonging to the other chains related to reference one by the screw axis 2<sub>1</sub>. Like in the case of **9**·0.5H<sub>2</sub>O, the chains of molecules are linked to each other by additional H-bonds between a hydrogen atom of the indole ring and a nitrogen atom of a cyano group (Figure 8a, Table 4). The angle between interpenetrating chains is about 84° (see Figure 8b).

As we have already mentioned, the crystal packing characteristics of compounds **9**·0.5H<sub>2</sub>O and **10** strongly resemble those we found for compounds **5** and **6**. In all these structures, the molecules form chains with big gaps between neighboring molecules. Interestingly, in these molecules only one hydrogen of the amino group (the “outsider” hydrogen) participates in the H-bond that links molecules into chains. The second H atom (the “insider” hydrogen) is not active in the H-bond formation, probably because it is too sterically shielded. In the case of structure **9**·0.5H<sub>2</sub>O, the only hydrogen bond it can really participate in is one with a small water molecule. Molecules in crystals **9**·0.5H<sub>2</sub>O and **10**, however, have other hydrogen atoms that can participate in the H-bond formation: those of water molecules and the H atom at the indole nitrogen, respectively. As a result, in the crystal structures of **9**·0.5H<sub>2</sub>O and **10**, the molecular chains are linked to each other by H-bonds, whereas in the case of compounds **5** and **6**, the chains are not linked.

In the **9**·0.5H<sub>2</sub>O and **10** crystals, we found molecular chains with gaps between translational molecules similar to those





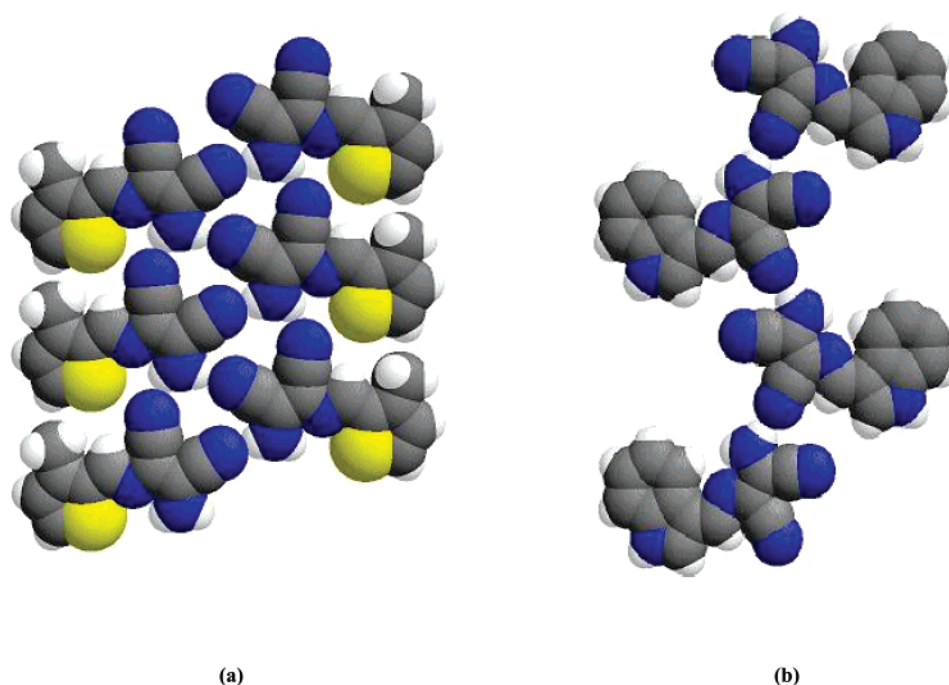
**Figure 9.** (a) Fragment of one chain in the crystal of ACNPH. (b) Mutual orientation of chains in the unit cell parallel to planes (012) and (012) for two different chains, respectively.

described in other research publications.<sup>23–29</sup> All compounds with the above-mentioned chain structure form acentric crystals, as well. In these articles, several conjugated hydrazones are described, as potential nonlinear optical compounds. All these hydrazones have a general structure D– $\pi$ –A with a nitro group acting as an acceptor moiety. Donor groups vary from halogens to alkoxy- to dialkylamino- substituents. It was reported, that all of these compounds have a  $\lambda$ -shaped packing motif due to formation of intermolecular H-bonds between an oxygen atom of the nitro group and a hydrogen atom of the NH-group of the phenylhydrazine residue; such molecular motifs cause acentric crystallization of the target hydrazones. It was reported that, in some cases, the molecular chains go along two diagonal crystallographic directions, very similar to the chains we found in crystals of our compounds **9**·0.5H<sub>2</sub>O and **10**. Because no

interpenetrated patterns in the crystals have been reported for these compounds in the original papers, we decided to review their crystal packings using published files with atomic coordinates. Indeed, after a careful examination of the crystal packings of the investigated hydrazones we found that all compounds of this type form some kind of interpenetrated crystal structure. For example, a fragment of one chain in the crystal of 4-(1-azacycloheptyl)benzaldehyde-4-(nitrophenyl)hydrazone (ACNPH), as well as the mutual orientation of two chains in the crystal lattice, are presented in Figure 9. In the crystal of ACNPH, which crystallizes in the acentric space group *Pca*2<sub>1</sub>, molecules form chains parallel to the (012) and (012) planes and form an interpenetrated structure that can be easily seen in Figure 9b. The molecular chains in the crystal of ACNPH are built by an operation that includes a glide plane *c*. The gaps in each chain are filled with the molecules belonging to the other chains related to the reference one by the glide plane *a*.

Overall, it could be said that formation of interpenetrated structures, rather than the  $\lambda$ -shaped packing motif itself, is responsible for the acentric crystallization of the investigated hydrazone derivatives.

A parallel could be drawn from the observation of the molecular packing characteristics of the present imine derivatives and compounds in our previous article.<sup>2</sup> We noticed that when a crystal contains H-bonded ribbons without any spaces between neighboring molecules (Figure 10a), crystallization in centrosymmetric space groups takes place. Compounds **7** and **7**·CH<sub>3</sub>CN, which form molecular ribbons with the above-mentioned type of structure, both crystallize in the centrosymmetric space group *P*2<sub>1</sub>/*c*. In our previous article,<sup>2</sup> two compounds (**3** and **4**) that form similar parquet-like ribbons, also crystallize in the centrosymmetric space groups *P*2<sub>1</sub>/*c* and *C*2/*c*, respectively. On the other hand, when the H-bonded chains have significant space between neighboring molecules (Figure 10b), we observed crystallization in the acentric space groups. Compounds **9**·0.5H<sub>2</sub>O and **10** form a pattern of interpenetrated chains in both crystals, and crystallize in the acentric space



**Figure 10.** (a) Space-filling model of a fragment of one molecular ribbon in crystal of **7**, (b) Space-filling model of one molecular chain in crystal of **10**.



groups *Fdd2* and *Pna2<sub>1</sub>*, respectively. In our previous article,<sup>2</sup> two compounds (**5** and **6**) that form similar interpenetrating molecular chains, also crystallize in the acentric space group *Pca2<sub>1</sub>*.

The reason for a different crystallization behavior between the centrosymmetric compounds **7** and **7**·CH<sub>3</sub>CN, and the acentric compounds **9**·0.5H<sub>2</sub>O and **10**, can be understood after examination of the H-bonded one-dimensional molecular associates: ribbons and chains. It is possible to see that molecular ribbons with a close molecular packing are usually coplanar to each other and packed in an antiparallel manner, giving a centrosymmetric structure. H-bonded chains with significant gaps between molecules create a compact molecular arrangement in the crystals by interpenetration of neighboring chains in the gaps, leading to their crossed orientation. So, the interpenetrating chain structures form an asymmetric arrangement.

#### 4. Conclusions

Our results show that the strategy of molecular and crystal structure design previously found for arylidene derivatives,<sup>2</sup> gave positive results for analogous heterocyclic imine derivatives, achieving elevated *T<sub>m</sub>* temperatures and acentric crystal packings. Introduction of an additional amino group in the acceptor moiety of all six molecules studied, in all cases resulted in H-bond formation and in a significant increase of *T<sub>m</sub>* of at least 60–70 deg (exceptions are the crystal hydrate and the solvate). For five of the compounds that have been considered, crystals suitable for X-ray analysis were grown and studied. In three of them, acentric structures were observed. It was found that, in the acentric crystal of **8**, H-bonds form a 3D network. The molecules of compounds **9** and **10** form, in their crystals, one-dimensional H-bonded head-to-head associates (chains). In both cases, an unusual interpenetrating packing of such chains in the crystal results in the formation of acentric structures. It is possible to conclude that, in this case, H-bonds that are favorable for the formation of an acentric pattern, are not suppressed by the influence of high dipole moments that usually result in antiparallel molecular orientation. The molecules in crystals **7**, **7**·CH<sub>3</sub>CN, and **12** form molecular one-dimensional H-bonded head-to-head associates (ribbons). These ribbons, however, overlap in such a manner that form centrosymmetric structures. We were able to find certain similarities between the crystal structures of the heterocyclic imines and the aromatic imines published in our preceding paper,<sup>2</sup> that put us one step closer to the solution of directional design of crystal packing in organic crystalline NLO compounds.

**Acknowledgment.** We gratefully acknowledge financial support of this research by NASA grant NAG8-1708, and NASA cooperative agreement NCC8-195-A.

**Supporting Information Available:** Atomic coordinates and molecular geometry parameters for compounds **3a–d** and **3f**

presented in X-ray crystallographic information (CIF). This material is available free of charge via the Internet at <http://pubs.acs.org>.

#### References and Notes

- (1) Gorman, C. B.; VanDoremale, G. H. J.; Marder, S. R. In *Molecular and Biomolecular Electronics. Advances in Chemistry Series 240*; Birge, R. R., Ed.; American Chemical Society: Washington, D.C, 1994; pp 195–202.
- (2) Nesterov, V. V.; Antipin, M. Yu.; Nesterov, V. N.; Penn, B. G.; Frazier, D. O.; Timofeeva, T. V. *Cryst. Growth Des.*, in press, 2004.
- (3) Kanis, D. R.; Ratner, M. A.; Marks, T. J. *Chem. Rev.* **1994**, *94*, 195.
- (4) Cheng, L.-T.; Tam, W.; Marder, S. R.; Stiegman, A. E.; Rikken, G.; Spangler, C. W. *J. Phys. Chem.* **1991**, *95*, 10643.
- (5) Jen, A. K.-Y.; Rao, V. P.; Wong, K. Y.; Drost, K. J. *J. Chem. Soc., Chem. Commun.* **1993**, 90.
- (6) Rao, V. P.; Jen, A. K.-Y.; Wong, K. Y.; Drost, K. J. *J. Chem. Soc., Chem. Commun.* **1993**, 1118.
- (7) Wong, K. Y.; Jen, A. K.-Y.; Rao, V. P.; Drost, K. J. *J. Phys. Chem.* **1994**, *100*, 6818.
- (8) Keshari, V.; Wijekoon, W. M. K. P.; Prasad, P. N.; Karna, S. P. *J. Phys. Chem.* **1995**, *99*, 9045.
- (9) Varanasi, P. R.; Jen, A. K.-Y.; Chandrasekhar, J.; Namboothiri, I. N. N.; Rathna, A. *J. Am. Chem. Soc.* **1996**, *118*, 12443.
- (10) Albert, I. D. L.; Marks, T. J.; Ratner, M. A. *J. Am. Chem. Soc.* **1997**, *119*, 6575.
- (11) Van Waalre, C. A.; Maarsman, A. W.; Flipse, M. C.; Jenneskens, L. W.; Smeets, W. J. J.; Spek, A. L. *J. Chem. Soc., Perkin Trans. 2* **1997**, 809.
- (12) Breitling, E. M.; Shu, C.-F.; McMahon, R. J. *J. Am. Chem. Soc.* **2000**, *122*, 1154.
- (13) Chetkina, L. A.; Gel'fand, I. M.; Ginzburg, S. L.; Neigauz, M. G.; Bepalov, B. P.; Dzyabchenko, A. V. *Kristallografiya*, **1983**, *28*, 470.
- (14) Chetkina, L. A.; Kurov, G. N.; Dmitrieva, L. L.; Sobolev, A. N. *Kristallografiya*, **1991**, *36*, 499.
- (15) Farrar, W. V. *Rec. Chem. Prog.* **1968**, *29*, 85.
- (16) Nesterov, V. N.; Timofeeva, T. V.; Borbulevych, O. Ya.; Antipin, M. Yu.; Clark, R. D. *Acta Crystallogr., Sect. C* **2000**, *56*, 971.
- (17) Enraf-Nonius 1989. CAD-4 Software. Version 5.0. Enraf-Nonius, Delft, The Netherlands.
- (18) Antipin, M. Yu.; Barr, T. A.; Cardelino, B. H.; Clark, R. D.; Moore, C. E.; Myers, T.; Penn, B.; Romero, M.; Sanghadasa, M.; Timofeeva, T. V. *J. Phys. Chem. B* **1997**, *101*, 2770.
- (19) Antipin, M. Yu.; Timofeeva, T. V.; Clark, R. D.; Nesterov, V. N.; Sanghadasa, M.; Barr, T. A.; Penn, B.; Romero, L.; Romero, M. *J. Phys. Chem. A* **1998**, *102*, 7222.
- (20) QCPE; MOPAC, Quantum Chemistry Program Exchange, Version 6, 1990.
- (21) Cardelino, B. H.; Moore, C. E.; Stickel, R. E. *J. Phys. Chem.* **1991**, *95*, 8645.
- (22) Cardelino, B. H.; Moore, C. E.; Frazier, D. O. *J. Phys. Chem. A* **1997**, *101*, 2207.
- (23) De Lucas, A. I.; Martin, N.; de Miguel, P.; Seoane, C.; Albert, A.; Cano, F. H. *J. Mater. Chem.* **1995**, *5*, 1141.
- (24) Allen, F. H.; Kennard, O.; Watson, D. G.; Brammer, L.; Orpen, A. G.; Taylor, R. *J. Chem. Soc., Perkin Trans. 2* **1987**, S1.
- (25) Brown, J. N.; Kutchan, T. M.; Rist, P. E. *Cryst. Struct. Commun.* **1980**, *9*, 17.
- (26) Serbutoviez, C.; Bosshard, C.; Knopfle, G.; Wyss, P.; Pretre, P.; Gunter, P.; Schenk, K.; Solari, E.; Chapuis, G. *Chem. Mater.* **1995**, *7*, 1198.
- (27) Wong, M. S.; Meier, U.; Pan, F.; Gramlich, V.; Bosshard, C.; Gunter, P. *Adv. Mater.* **1996**, *8*, 416.
- (28) Wong, M. S.; Gramlich, V.; Pan, F.; Bosshard, C.; Gunter, P. *Acta Crystallogr., Sect. C (Cryst. Struct. Commun.)* **1997**, *53*, 757.
- (29) Wong, M. S.; Gramlich, V.; Bosshard, C.; Gunter, P. *J. Mater. Chem.* **1997**, *7*, 2021.